JOURNAL OF THERMOPHYSICS AND HEAT TRANSFER
Vol. 12, No. 2, April–June 1998

Performance of Liquid Metal Heat Pipes During a Space Shuttle Flight

Timothy J. Dickinson*
U.S. Air Force Institute of Technology, Wright–Patterson Air Force Base, Ohio 45433
W. Jerry Bowman†
Brigham Young University, Provo, Utah 84602
and
Marko Stoyanof‡
U.S. Air Force Phillips Laboratory, Kirtland Air Force Base, New Mexico 87117

This study investigated liquid metal heat pipe performance in a microgravity environment. Three stainless-steel/potassium heat pipes were flown on Space Shuttle mission STS-77 in May 1996. The objectives of the experiment were to characterize the frozen startup and restart transients, to compare the flight and ground test data to establish a performance baseline for analytical model validation, and to assess the three different heat pipe designs. Microgravity operation did not adversely impact the startup or restart behavior of the heat pipes. The heat pipes operated within the predicted performance envelopes. The three designs had distinct startup characteristics, yet were similar in steady-state performance. These results will serve as a benchmark for further liquid metal heat pipe studies and space system applications.

Introduction

PERFORMANCE characteristics of liquid metal heat pipes are not established for microgravity operation. Although model analyses and ground tests predict the performance of these heat pipes, the results have not been verified by microgravity tests. Ground tests reveal startup from the frozen state as the critical phase of operation because condensed liquid may freeze in the condenser and lead to evaporator dryout. In terrestrial applications, gravity can assist in the return of condensed fluid to the evaporator when the evaporator is positioned below the condenser, thus minimizing dryout risk. Space systems, however, do not have this advantage, and it has been assumed until now that startup may prove a significant challenge because liquid flow relies solely on the capillary pumping ability of the wick. Because the simulation of a microgravity environment or prediction of its effects is difficult to achieve on Earth, flight tests in low Earth orbit are essential to adequately quantify the performance of liquid metal heat pipes in this unique environment.[1–4]

Three stainless-steel/potassium heat pipes were designed, manufactured, integrated, and recently tested during a Space Shuttle mission. This investigation responds to the requirements of various organizations within the Department of Defense, NASA, and industry. Three research objectives were established to meet these requirements:

1) Characterize the frozen startup and restart behavior of liquid metal heat pipes in a microgravity environment.

2) Compare microgravity and ground test results to establish a performance baseline for future analytical model validation.

3) Assess the performance of three heat pipe designs.

Liquid metal heat pipe behavior in a microgravity environment is not well understood.[2] Heat pipe scientists and engineers require microgravity performance data to provide this knowledge and to benchmark analytical models.[5] Achievement of the first two objectives will meet this requirement. Numerous wick designs exist for liquid metal heat pipes. The optimum structures for microgravity operation are unknown.[2] Fulfillment of the third objective provides this necessary information to heat pipe designers.

Experimental Design and Setup

General design parameters of the heat pipe components are described next. Critchley and Corrigan[2] and Dickinson[6] provide a more detailed description of the individual components and the integrated experimental platform.

The heat pipe containers were constructed of type 304 stainless steel. Each heat pipe had the same external dimensions: 61.0 cm length, 2.30 cm o.d., and 0.089 cm wall thickness. The length was divided into an 8.9-cm evaporator and a 52.1-cm condenser; an adiabatic section was not present.[7] The wicks were also constructed of type 304 stainless steel. The three wick structures were homogeneous, annular gap, and arterial, as illustrated in Fig. 1.[7]

All three wick designs have a high effective thermal conductivity because the working fluid is a liquid metal. The homogeneous wick structure, a simple, classic design, serves as a baseline for comparison against other designs. It excels in capillary pumping ability because of the fine pores at the wick surface, but offers low permeability. The annular gap wick retains favorable capillary pumping ability, but also provides increased permeability because of the unimpeded flow path for condensed fluid. However, annular gap wick designs may encounter priming difficulties during startup. The arterial wick structure also combines high capillary pumping ability and high permeability. The disadvantage of this structure is the potential for vapor bubble formation in the arteries during startup; vapor bubbles are difficult to collapse and may prevent the return of condensed liquid.[8]

The homogeneous wick was composed of 11 layers of 100 mesh screen and was 0.23 cm thick. The annular gap and arterial wicks were composed of four layers of 250 mesh screen and were 0.03 cm thick. The annular gap wick had a 0.10-cm annulus, defined as the maximum distance between the wick and container wall. The arterial wick had two 0.10-cm-diam arteries positioned 180 deg apart.[7]

Received April 28, 1997; revision received Nov. 10, 1997; accepted for publication Dec. 4, 1997.

*Graduate Student, Department of Aeronautics and Astronautics.

†Associate Professor, Mechanical Engineering Department.

‡Focused Technology Area Lead, Satellite Thermal Control.

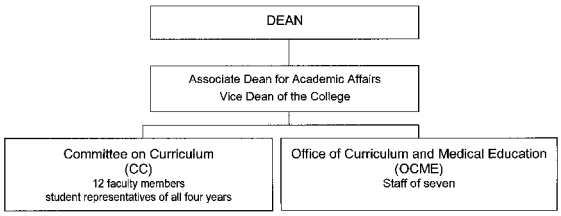

Fig. 1 Wick structure designs.

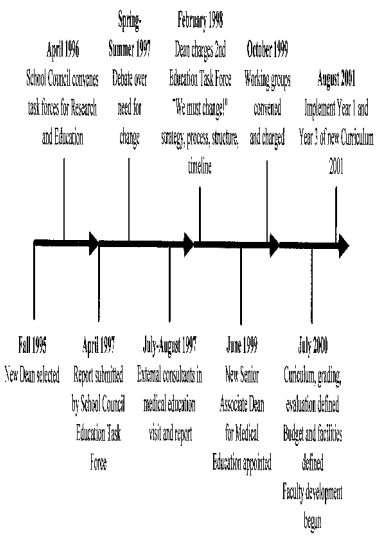

Fig. 2 Experimental platform.

Each of the heat pipes was charged with potassium. Potassium was selected because its operating temperature range of 250–1500°C can accommodate many requirements of future spacecraft technologies. The intended amount of working fluid allows complete saturation of the wick during operation and provides a 2.0-cm pool of reserve liquid in the condenser to protect against evaporator dryout. Based on these two conditions, the homogeneous, annular gap, and arterial wicks required 44.0, 42.7, and 17.3 g of potassium, respectively.[7] The amounts of potassium distilled into the heat pipes were 46.0, 61.5, and 19.2 g for the homogeneous, annular gap, and arterial wick designs, respectively. The homogeneous and arterial wick heat pipes were overcharged by 4.5 and 11.0%. The annular gap wick heat pipe, however, received a significant 44.0% excess.[9]

The heat pipes were mounted on an aluminum experimental support frame, as shown in Fig. 2. The mounting flange of each heat pipe, attached to the evaporator end cap, was cantilevered to the top end plate of the support frame. Ceramic spacers insulated the top end plate from the heat pipes. The condenser end caps were secured to the bottom end plate with ceramic glass sockets. The sockets provided insulation, prevented lateral motion, and allowed axial expansion and contraction of the pipes.[10]

Helical nichrome resistance heaters were attached to the evaporator and condenser of each heat pipe. The heaters had a radial thickness of 0.4 cm; the lengths were 8.9 and 7.6 cm, respectively.[2,10] The heaters were fixed to the heat pipes with stainless-steel jackets; the heaters and jackets are shown in Fig. 3. The evaporator end of each heat pipe was inserted into a stainless-steel cylindrical enclosure. Radiation losses from the evaporator heater were minimized with seven layers of molybdenum shielding. Conductive losses from the enclosure were minimized with ceramic spacers between the enclosure and top end plate.[10]

Component temperatures were obtained with type K thermocouples. Heat pipe temperatures were monitored with 24 thermocouples: 16 along the condenser between the evaporator

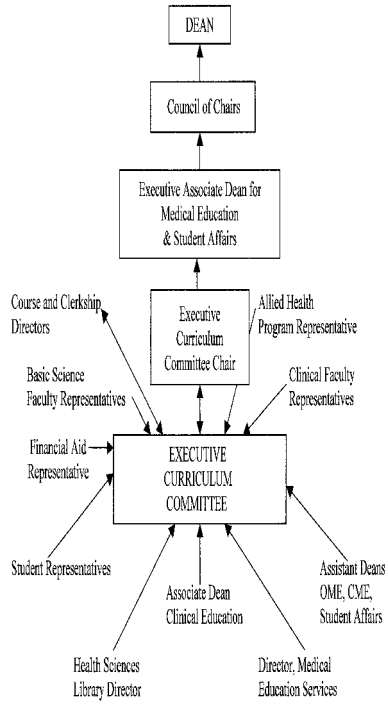

Fig. 3 Heat pipe heaters: a) evaporator heater with jacket and b) condenser heater with jacket removed.

enclosure and condenser heater, and four on each evaporator and condenser heater jacket.

The 59-kg experimental platform was installed in an uninsulated NASA Hitchhiker flight canister. A butterfly vent valve, located on the canister bottom plate, opened while in orbit to achieve the required 10^{-4} torr vacuum to ensure negligible convection heat transfer; heat output from the pipes was limited to radiation. The canister was mated to a Hitchhiker bridge prior to integration with the orbiter Endeavour.

Preflight Characterization

Faghri[8] discusses seven heat transfer limitations applicable to liquid metal heat pipes. Three of the seven are commonly encountered during heat pipe startup but do not represent operational failure: vapor continuum, viscous, and sonic limits. Another three, however, represent failure of the heat pipe: capillary, entrainment, and boiling limits. The final limitation is the frozen startup limit.[11] If the condensation rate of vapor onto frozen working fluid exceeds the melt rate of working fluid, the evaporator will become depleted. The ratio of the latter to the former must exceed unity for successful startup. These limits were calculated for each of the three heat pipes and will be compared later with the test results.

Los Alamos National Laboratory tested the heat pipes individually in a vacuum chamber prior to delivery. Each pipe experienced two startup and shutdown cycles. A 350-W step input was applied to the evaporator by a radio frequency induction heater, and heat removal was continuously monitored with a water-cooled calorimeter. The temperature profiles were consistent with heat pipe startup theory.[1]

U.S. Air Force Phillips Laboratory also conducted thermal proof tests of the individual heat pipes prior to integration and thermal vacuum tests. The pipes were operated horizontally in a vacuum chamber. A resistance heater coupled to the evaporator provided stepped power increments up to 304 W. The heat transfer environment was confined to radiation exchange between the heat pipe and test chamber; the walls of the chamber were maintained at room temperature. These temperature profiles were similar to the Los Alamos test results.[12]

Thermal vacuum tests[13] were conducted by U.S. Air Force Phillips Laboratory. The objective of the tests was operational

verification of the heat pipes and experimental control unit in the expected flight environments. The platform was tested in the fully integrated flight configuration with the heat pipes in a horizontal position to minimize gravity effects. The tests were conducted at vacuum pressures between 10^{-8} and 10^{-6} torr to restrict heat output to radiation between the pipes and canister walls. Each heat pipe cycled twice through a startup and shutdown scenario. The startup scenario was initiated by a 30-min thaw period to melt the frozen potassium in the evaporator; the evaporator heater operated for 15 min at heater power levels of 80 and 135 W. A 15-min ramp to the maximum power of 280 W followed the thaw period. A heater power of 280 W was maintained for 45 min until steady-state operation was achieved. Power was then removed from the heater and the heat pipe cooled for 4 h. All experimental control unit components performed as designed. Heat pipe operation appeared consistent with theory.

Test Execution

The three experimental objectives led to the development of three test scenarios: the objectives were characterization of startup behavior, comparison of microgravity and ground performance, and assessment of three heat pipe designs. All tests began from the frozen state.

Three startup characterization test senarios addressed the first two experimental objectives. The first test, titled Startup, was a repeat of the thermal vacuum tests described earlier. The other two tests resulted from the work of Jang et al.[14] The numerical results of their mathematical model highlight two important findings: a small amount of heat input at the condenser aids startup from the frozen state and a starved evaporator prevents a successful startup. The second and third tests, titled Preheated Condenser and Starved Evaporator,[15] investigated these two issues.

The Startup test incorporated the same heat input profile as the thermal vacuum tests. The results established the baseline for startup characterization of the heat pipes and provided a comparison between ground and flight test data. This test was conducted twice on each heat pipe to assess performance repeatability.

The Preheated Condenser test investigated the effect of heat input at the condenser prior to startup. A power of 65 W applied to the condenser heater for 90 min fully melted the potassium in that section. Power was then removed from the condenser heater, and the heat pipe entered the Startup test profile.

The third objective was addressed through a series of steady-state tests at seven heater power levels: 80, 105, 135, 165, 200, 240, and 280 W. Continuum front advancement was observed and compared for each of the heat pipes at the various levels. Operation at these low-power levels revealed the minimum power required for each heat pipe to achieve an isothermal, or fully operational, condition.

During the Space Shuttle flights, the platform operated continuously for 200 h. Operations continued during shuttle stationkeeping and satellite rendezvous maneuvers. A thermistor positioned in the canister below the experimental platform recorded temperatures between 10 and 35°C, consistent with payload bay temperatures. Canister pressures were maintained between 5×10^{-6} and 5×10^{-5} torr.[2]

Flight and Ground Test Results

Experimental results and analyses are grouped by experimental objective. Experimental data consisted of heater and heat pipe wall temperatures as a function of time for the various test scenarios.

Objective 1: Startup Characterization

The two thermocouples at each end of the heat pipes are located on the evaporator and condenser heater jackets and therefore do not reflect actual heat pipe wall temperatures.

Startup Test

Heat pipe wall temperature profiles for this test are illustrated in Fig. 4. The startup behavior of the homogeneous wick heat pipe was consistent with theory.[16] The continuum front, marked by the sharp temperature gradient, did not advance until vapor in the evaporator exceeded the continuum flow transition temperature of 313°C. Heat transfer between the evaporator and condenser was limited prior to advancement of the front because of the rarefied flow condition beyond the front. Heat transfer increased as the continuum front propagated along the condenser. After 30 min, the front had advanced 18 cm past the evaporator exit. The continuum front continued its progression toward the end of the condenser during the startup transient. The heat pipe was nearly isothermal between the evaporator exit and continuum front throughout the test; the temperature drop was typically 10–15°C.

The annular gap wick heat pipe was equally responsive to startup from the frozen state. The continuum front advanced after vapor exceeded the transition temperature of 305°C in the evaporator. This advancement is shown in Fig. 4b. Advancement of the front initially occurred more rapidly than in the other two heat pipes. After 30 min, the front was located 24 cm past the evaporator exit compared to 18 and 14 cm for the homogeneous and arterial wick heat pipes, respectively. After the potassium was completely melted, vapor swept the excess fluid to the end of the condenser; however, this behavior was anticipated.[16] The pool of excess fluid limited the effective length of the condenser to 37 cm, and the liquid is evidenced by the temperature drop at the end of the condenser. The temperature drop is a result of the long conduction path of the liquid. The stationary location of the temperature gradient near the end of the startup transient indicates the boundary of the excess fluid. A liquid pool length of 14 cm corresponds to

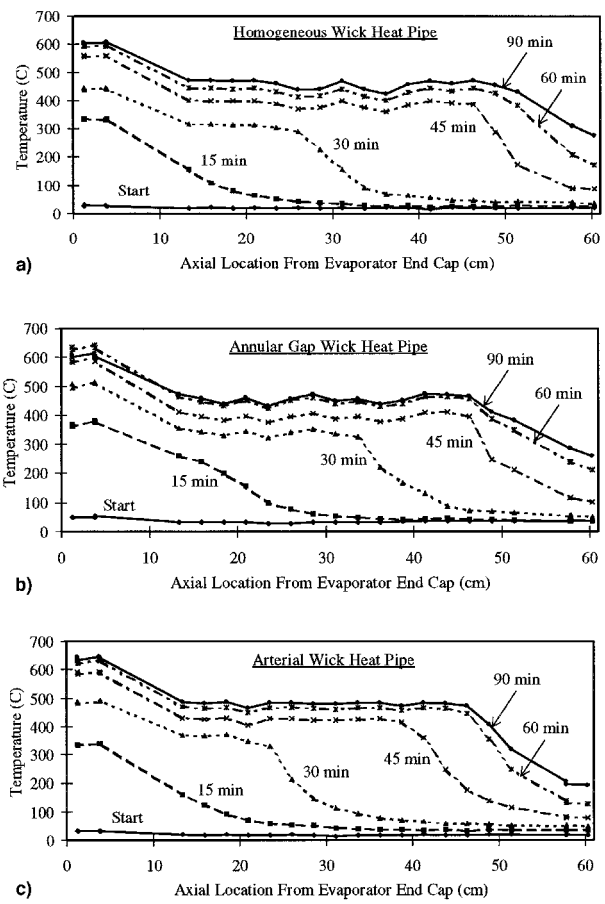

Fig. 4 Startup test temperature profiles.

excess liquid mass calculations as well as ground test observations.[1]

The startup behavior of the arterial wick heat pipe is shown in Fig. 4c. Advancement of the continuum front began after the vapor reached the transition temperature of 303°C. The front progressed steadily along the condenser and extended 37 cm past the evaporator exit at the end of the startup transient.

These tests were conducted twice to examine repeatability. The temperature profiles shown in Fig. 4 were duplicated for each heat pipe in the subsequent tests.

Preheated Condenser Test

Temperature profiles for this test are compared with those of the Startup test in Fig. 5. In all of the heat pipes, the potassium was completely melted in the condenser prior to initiation of the startup profile; heat pipe wall temperatures were 350°C near the condenser heater and 80 to 100°C near the evaporator. In this test, the heat pipe condenser was warmer throughout the startup transient. Advancement of the continuum front initially exceeded that of the Startup test scenario. The temperature profiles of the two scenarios coincide after 45 min for the homogeneous and annular gap wick designs and after 30 min for the arterial wick design. A preheated condenser accelerated startup initially but did not affect the steady-state condition or the time required to achieve it.

Shutdown Temperature Profile

Shutdown of the heat pipes was monitored to determine the distribution of potassium at ambient temperature. Each heat pipe cooled from a temperature of approximately 500 to 100°C in two hours. The heat pipes were nearly isothermal as the potassium in the condenser reached the solidification temperature of 64°C. The temperature difference between the evaporator and condenser ranged from 4 to 28°C for the three heat pipes. The time delay between solidification of potassium in the condenser and evaporator ranged from 12 to 40 min, with solidification occurring first in the condenser region. These time delays and low temperatures result in a maximum migration of 3 μg of potassium from the evaporator after solidification began in the condenser. This behavior occurred in all tests and indicated the working fluid was uniformly distributed in the frozen state.

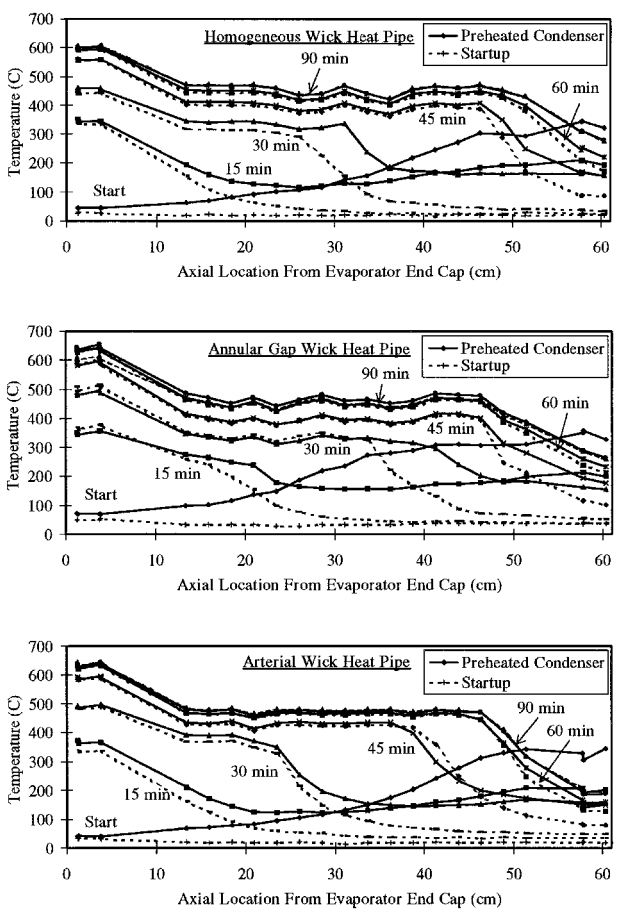

Fig. 5 Startup test vs preheated condenser test temperature profiles.

Restart

Each heat pipe experienced a minimum of nine thermal cycles, with all cycles initiated from the frozen state. The startup behavior was consistent in each scenario. These observations testify to the robustness of the heat pipes under these conditions as well as the repeatability in their performance.

Frozen Startup Limitation

As defined earlier, the ratio of melt rate to vapor freeze rate must exceed unity for successful startup. The values for the homogeneous, annular gap, and arterial wick designs are 6.7, 12.3, and 4.3, respectively. These values indicate robustness regarding startup behavior of the heat pipes. Experimental results support this prediction. The heat pipes did not experience difficulties during startup from the frozen state in any of the tests. This startup behavior is consistent with that of other liquid metal heat pipes during ground experiments.[17,18] The large thermal conductivity of liquid metals allows the fluid to melt by conduction before significant evaporation of the liquid occurs.

Objective 2: Flight and Ground Performance Comparison

Flight vs Ground Startup

A partial loss of ground thermal vacuum test data prevented complete startup characterization prior to the flight test. However, data were obtained at several points during the ground startup of each heat pipe. These thermal vacuum data are compared with the flight data in Fig. 6. Data from both tests were available at 5, 20, and 65 min for the homogeneous wick heat pipe, and 10, 25, and 55 min for the annular gap and arterial wick designs.

The flight performance of the homogeneous and arterial wick heat pipes compared favorably with ground thermal vacuum performance. Only the startup temperature profiles for the annular gap wick design were significantly different. The ground thermal vacuum test data are inconsistent with heat pipe theory, thermal proof test data, and flight-test data. The temperature profile at 25 min does not exhibit a sharp gradient and thus indicates the absence of a continuum front. Also, the profile at 55 min does not indicate the presence of excess working fluid pooled in the condenser. This pool was observed during all subsequent flight tests as well as the preceding thermal proof tests at Los Alamos National Laboratory[1] and U.S. Air Force Phillips Laboratory.[12] The lack of further ground test data prevents a complete assessment of the discrepancies; however, the differences are likely because of altered test conditions, such as an uneven distribution of working fluid. Further investigation is required to resolve these discrepancies.

Flight vs Ground Shutdown

The first flight test scenario was a steady-state test initiated with a 105-W step input. This test was repeated in the final series of flight tests. The first execution was preceded by a shutdown under the influence of gravity at the end of the ground thermal vacuum test. This shutdown probably resulted in pooling of the liquid along the bottom of the heat pipe and an uneven circumferential distribution of frozen potassium. The final execution was preceded by a shutdown without the influence of gravity and most likely resulted in an even distribution of the fluid about the circumference. However, if the

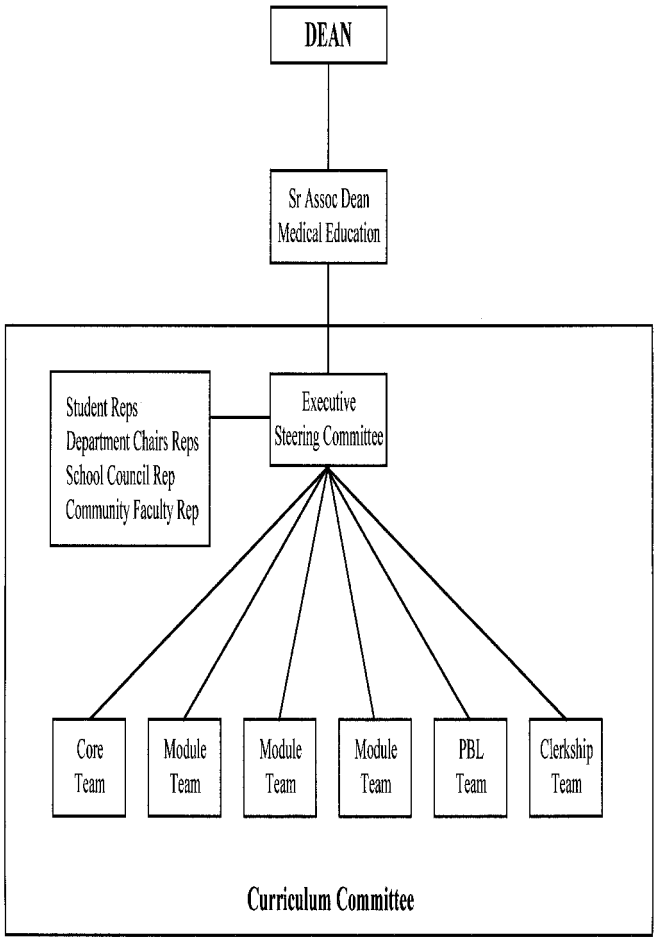

Fig. 6 Flight vs ground startup test temperature profiles.

different distributions did occur, they did not affect subsequent startup behavior. The startup temperature profiles were identical for both tests of all three heat pipe designs.

Objective 3: Design Assessment

Calculations of heat pipe energy throughput and evaporator and condenser temperatures led to the calculation of thermal resistance values for the heat pipes. General steady-state behavior and operation with respect to the predicted performance envelopes were also investigated.

Energy Throughput

Evaporator heater efficiencies were calculated for the seven steady-state power levels to determine heat pipe energy throughput. The heat loss from the heater was determined by a two-surface enclosure radiation analysis. The energy transmitted through each pipe was calculated by subtraction of this heat loss from the heater power. Dickinson[6] provides a detailed discussion of this analysis. Heater efficiencies ranged from 72 to 84% for the three heat pipes and seven power levels with a maximum standard deviation of 4.2%.

Evaporator Temperatures

Evaporator wall temperatures were determined from heater-jacket temperatures, heater power, heater efficiency, and contact resistances. The heater element was treated as a two-dimensional radial conduction problem with thermal energy generation. Dickinson[6] discusses this problem in detail. Solution of this problem allowed for calculation of the evaporator wall temperatures; calculations were made for the seven steady-state power levels. These temperatures were typically 20–60°C lower than the measured heater-jacket temperatures for the range of heater powers. The evaporator wall temperatures were required for the thermal resistance calculations.

Condenser Temperatures

All performance calculations were based on the effective condenser length defined by the location of the sharp temperature gradient at the continuum front. Condenser temperatures were treated as the average wall temperature along the effective length. Because the effective condenser did not include the region beneath the condenser heater in any of the test scenarios, calculation of wall temperatures beneath the condenser heaters was not required.

Heat Pipe Thermal Resistances

Thermal resistance of an object is defined as the ratio of temperature drop to energy transmitted. Theoretical and experimental thermal resistances were calculated for the heat pipes.

The theoretical resistances for each segment were calculated from Chi's[16] relations and verified with the approach of Dunn and Reay.[19] The thermal resistances associated with evaporation and condensation were two orders of magnitude less than the other resistances and were therefore neglected. Theoretical resistance calculations for the homogeneous wick heat pipe are 0.052°C/W at 300°C and 0.026°C/W at 500°C. The reduction in resistance for increased temperature occurs for two reasons. The wall and wick resistances of the condenser decrease by a factor of two because of the increased effective condenser length. The vapor resistance decreases by two orders of magnitude because of the higher vapor density associated with increased temperature. For these thermal resistances, a maximum temperature drop of 3°C through the wall and wick is predicted at the maximum heater power of 280 W. This small temperature drop substantiates the approximation of vapor temperatures with wall temperatures.

Heat pipe experimental resistances were calculated for the seven steady-state power levels and plotted as a function of heat transport rate in Fig. 7. These resistances were calculated as $R = (T_{evap} - T_{cond})/(P_{HTR}\eta_{HTR})$, where T_{evap} was the calculated evaporator temperature, T_{cond} was the averaged measured condenser temperature, P_{HTR} was the power input into the heater, and η_{HTR} was the efficiency of the heater. Experimental thermal resistances during flight were between 0.83 and 1.93°C/W for an initial transmitted power of 60 W. The experimental resistance of the annular gap wick heat pipe was initially significantly higher than the other two designs because of excess working fluid pooled along the heat pipe. This excess resulted in a longer conduction path through the wick. The excess fluid was forced to the end of the condenser as it melted, and the decrease of liquid in the remainder of the heat pipe decreased the resistance through the wick.[16]

The resistance of each heat pipe decreased as the heat load and effective condenser length increased and the heat pipe became fully operational. These observations are consistent with those made by Brennan and Kroliczek.[20] The resistance values for the homogeneous, annular gap, and arterial wick heat pipes at a maximum transmitted power of 225–235 W were 0.38,

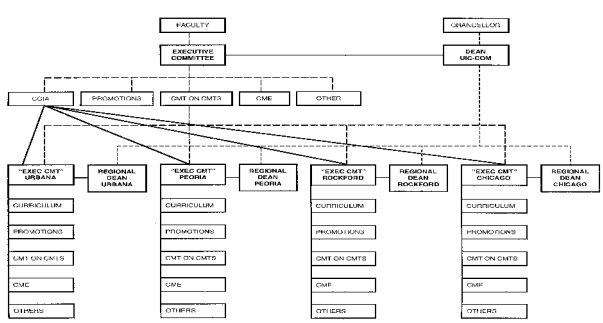

Fig. 7 Heat pipe thermal resistances.

0.55, and 0.42°C/W, respectively. The resistances became less dependent on heat load as the continuum front stabilized near the end of the condenser. While the homogeneous wick design appears to have the advantage of lowest thermal resistance, the differences become insignificant from a design consideration at the higher heat transport levels.

Steady-State Tests

Performance of the homogeneous wick design was consistent with theory. As the heat input increased, the temperature increased and the continuum front progressed along the condenser. The location of the continuum front was marked by the sharp temperature gradient. Steady-state temperature profiles for the seven heater power levels are provided in Fig. 8.

The annular gap wick heat pipe functioned as the homogeneous wick heat pipe up to a heater power of 165 W. Further heat load increases raised the isothermal temperature of the annular gap wick heat pipe, but the excess working fluid prevented an increase in effective condenser length. The length of the inactive zone corresponds to excess fluid volume calculations. This phenomenon was also observed during thermal proof tests at Los Alamos National Laboratory[1] and U.S. Air Force Phillips Laboratory.[12]

Operation of the arterial wick heat pipe was also consistent with theory. Advancement of the continuum front for increased power levels occurred in shorter increments compared to the other heat pipes. Initial condenser length was 9 cm for an 80-W heater power, compared to 22 and 25 cm for the homogeneous and annular gap wick heat pipes, respectively. The condenser length approached that of the homogeneous wick heat pipe at the maximum heater power of 280 W. The lengths were 37 and 42 cm, respectively.

This behavior of the arterial wick heat pipe was also observed by U.S. Air Force Phillips Laboratory during thermal proof tests. At that time, the presence of noncondensible gas (NCG) was suspected as the cause of the behavior.[12] However, several facts indicate that NCG was probably not present. This behavior was not observed during thermal proof tests at Los Alamos National Laboratory.[1] Therefore, if NCG were present, it must have been introduced after heat pipe manufacture. Leakage and corrosion are the most probable processes of NCG generation. All three heat pipes passed leak checks by Los Alamos National Laboratory[9] and OAO Corporation.[10] In life tests at Los Alamos, a similar type 304 stainless-steel/potassium heat pipe operated at 600°C for 8000 h without degradation. Therefore, the most probable explanation for this behavior is not NCG but rather insufficient heater power for further continuum front advancement. The Los Alamos thermal proof test was conducted at a transmitted power of 350 W while the U.S. Air Force Phillips Laboratory and flight tests were conducted at maximum transmitted powers of 253 and 236 W, respectively. Advancement of the continuum front to the end of the condenser, as observed in the Los Alamos test, is anticipated as well if the heat input of the other tests had been increased to 350 W.

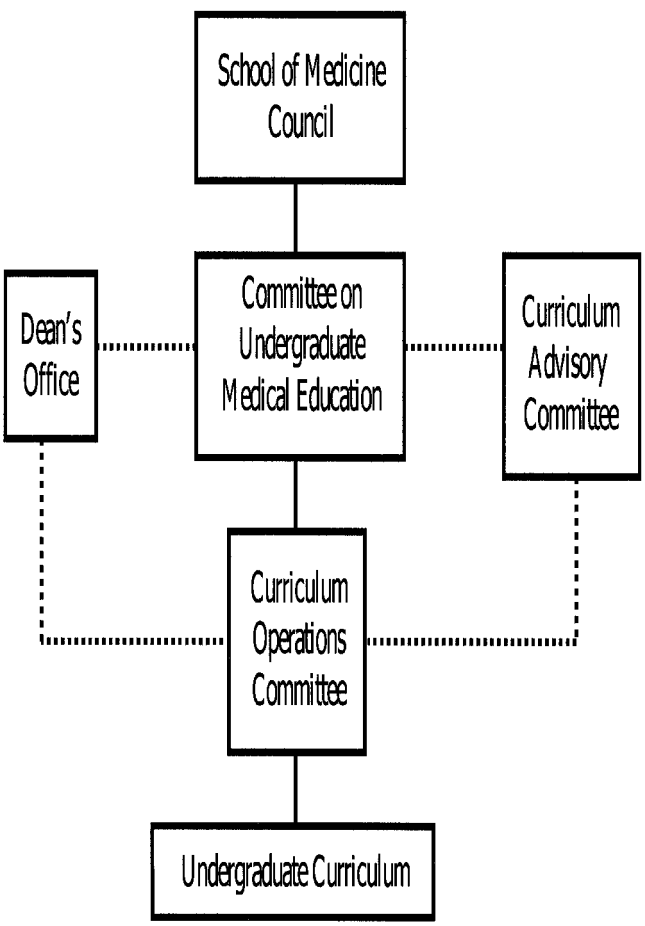

Fig. 8 Steady-state test temperature profiles.

Conclusions and Recommendations

The first experimental objective was characterization of the frozen startup and restart behavior of liquid metal heat pipes in a microgravity environment. The results of the startup tests successfully characterized this behavior. Startup was consistent with theory. The continuum front, marked by a sharp temperature gradient, advanced steadily after the establishment of vapor continuum flow. The heat pipe wall was isothermal between the evaporator exit and continuum front. The heat pipes cooled isothermally to provide an even distribution of frozen working fluid after heat pipe shutdown.

Numerous starts from the frozen state demonstrated consistent restart behavior. A preheated condenser initially accelerated startup but did not affect the steady-state condition or the time required to achieve it. The robustness predicted by the frozen startup limit calculation for these test conditions was confirmed with experimental results.

The second objective was to compare microgravity performance with ground test performance. The experimental results indicate that homogeneous and arterial wick heat pipe performances were insensitive to gravity effects. For these heat pipes, microgravity performance closely matched ground thermal vacuum performance, including startup transient and steady-state behavior. The discrepancies between the ground and flight data for the annular gap wick heat pipe are unresolved. Further investigation is required to determine any potential differences between terrestrial and microgravity performance.

The third objective was performance assessment of three heat pipe designs. Each of the three designs had unique strengths. The homogeneous wick heat pipe had a smaller thermal resistance, the annular gap wick heat pipe started more quickly, and the arterial wick heat pipe had the largest theoretical performance margin.

The experimental data and results of this study are available for validation of liquid metal heat pipe startup transient models. Validation and improvement of these critical tools will assist in the design of future systems. Accurate performance predictions of liquid metal heat pipe startup behavior are required to build reliable and efficient thermal control systems for high-temperature space applications.

Recommendations for future micro-*g* experiments include operation throughout a larger power range and increased thermal coupling between the condenser and surroundings. The first condition allows investigation of a larger portion of the performance envelope. The second condition could maintain frozen working fluid in the condenser and lead to better examination of startup difficulties.

Acknowledgment

This investigation was sponsored by the U.S. Air Force Phillips Laboratory.

References

[1]Woloshun, K. A., Merrigan, M. A., Sena, J. J., and Critchley, E., "High Temperature Heat Pipe Experiments in Low Earth Orbit," American Society of Mechanical Engineers, Paper 93-HT-23, New York, Aug. 1993.

[2]Critchley, E. P., and Corrigan, M. E. "Design of a Liquid Metal Heat Pipe Space Experiment," *12th Symposium on Space Nuclear Power and Propulsion*, American Inst. of Physics, New York, Jan. 1995, pp. 145–154.

[3]"Liquid Metal Thermal Experiment Point Paper," U.S. Air Force Phillips Lab., Materiel Command, Kirtland AFB, NM, 1996.

[4]Peterson, G. P., *An Introduction to Heat Pipes: Modeling, Testing and Applications*, Wiley, New York, 1994.

[5]Tournier, J.-M. P., and El-Genk, M. S., "HPTAM, A Two-Dimensional Heat Pipe Transient Analysis Model, Including the Startup From a Frozen State," Inst. for Space and Nuclear Power, Univ. of New Mexico, College of Engineering, NASA Lewis Research Center Grant NAG3-941, Final Rept. UNM-ISNPS-2-1996, Albuquerque, NM, May 1996.

[6]Dickinson, T. J., "Performance Analysis of a Liquid Metal Heat Pipe Space Shuttle Experiment," M.S. Thesis, U.S. Air Force Inst. of Technology, Dayton, OH, Dec. 1996.

[7]"Heat Pipe Final Designs," Los Alamos National Lab., Los Alamos, NM, April 1992.

[8]Faghri, A., *Heat Pipe Science and Technology*, Taylor and Francis, Washington, DC, 1995.

[9]"Heat Pipe Fabrication Procedures," Los Alamos National Lab., Los Alamos NM, June 1992.

[10]"Liquid Metal Thermal Experiment Phase III Flight Safety Data Package," U.S. Air Force Phillips Lab., Materiel Command, Kirtland AFB, NM, Dec. 1995.

[11]Cao, Y., and Faghri, A., "Closed-Form Analytical Solutions of High-Temperature Heat Pipe Startup and Frozen Startup Limitation," *Journal of Heat Transfer*, Vol. 114, Nov. 1992, pp. 1028–1035.

[12]"Memorandum for Record Regarding Thermal Proof Test of Liquid Metal Thermal Experiment," U.S. Air Force Phillips Lab., Materiel Command, Kirtland AFB, NM, Aug. 1995.

[13]"Liquid Metal Thermal Experiment Thermal Vacuum Test Plan," U.S. Air Force Phillips Lab., Materiel Command, Kirtland AFB, NM, Aug. 1995.

[14]Jang, J. H., Faghri, A., Chang, W. S., and Mahefky, E. T., "Mathematical Modeling and Analysis of Heat Pipe Startup from the Frozen State," *Journal of Heat Transfer*, Vol. 112, Aug. 1990, pp. 586–594.

[15]Keddy, M. D., Merrigan, M. A., and Critchley, E., "Modeling the Mass Migration Phenomena in Partially Frozen Heat Pipes," *Proceedings of the 11th Symposium on Space Nuclear Power and Propulsion*, Inst. for Space Nuclear Power Studies, Albuquerque, NM, 1994, pp. 989–995.

[16]Chi, S. W., *Heat Pipe Theory and Practice*, Hemisphere, Washington, DC, 1976.

[17]Deverall, J. E., Kemme, J. E., and Florschuetz, L. W., "Sonic Limitations and Startup Problems of Heat Pipes," Los Alamos Scientific Lab., Rept. LA-4518, Los Alamos National Lab., Los Alamos, NM, Nov. 1970.

[18]Jang, J. H., "A Study of Startup Characteristics of a Potassium Heat Pipe from the Frozen State," *Journal of Thermophysics and Heat Transfer*, Vol. 9, No. 1, 1995, pp. 117–122.

[19]Dunn, P. D., and Reay, D. A., *Heat Pipes*, 4th ed., Elsevier, New York, 1994.

[20]Brennan, P. J., and Kroliczek, E. J., *Heat Pipe Design Handbook*, Vol. 1, B & K Engineering, Inc., Towson, MD, 1979.